Solder Joint Reliability of Pb-free Sn-Ag-Cu Ball Grid Array (BGA) Components in Sn-Pb Assembly Process

Robert Kinyanjui, Ph.D.
Technology Development Center
Sanmina-SCI Corporation
robert.kinyanjui@sanmina-sci.com

Quyen Chu
Jabil
quyen_chu@jabil.com

Polina Snugovsky, Ph.D.
Celestica Inc.
Toronto, ON, Canada
polina@celestica.com

Richard Coyle, Ph.D.
Alcatel-Lucent
Murray Hill, NJ
rcoyle1@alcatel-lucent.com

Abstract
For companies that choose to take the Pb-free exemption under the European Union's RoHS Directive and continue to manufacture tin-lead (Sn-Pb) electronic products, there is a growing concern about the lack of Sn-Pb ball grid array (BGA) components. Many companies are compelled to use the Pb-free Sn-Ag-Cu (SAC) BGA components in a Sn-Pb process, for which the assembly process and solder joint reliability have not yet been fully characterized.

A careful experimental investigation was undertaken to evaluate the reliability of solder joints of SAC BGA components formed using Sn-Pb solder paste. This evaluation specifically looked at the impact of package size, solder ball volume, printed circuit board (PCB) surface finish, time above liquidus and peak temperature on reliability. Four different BGA package sizes (ranging from 8 to 45 mm^2) were selected with ball-to-ball pitch size ranging from 0.5mm to 1.27mm. Two different PCB finishes were used: electroless nickel immersion gold (ENIG) and organic solderability preservative (OSP) on copper. Four different profiles were developed with the maximum peak temperatures of 210^{o}C and 215^{o}C and time above liquidus ranging from 60 to 120 seconds using Sn-Pb paste. One profile was generated for a lead-free control. A total of 60 boards were assembled. Some of the boards were subjected to an as-assembled analysis while others were subjected to an accelerated thermal cycling (ATC) test in the temperature range of -40^{o}C to 125^{o}C for a maximum of 3500 cycles in accordance with IPC 9701A standard. Weibull plots were created and failure analysis performed.

Analysis of as-assembled solder joints revealed that for a time above liquidus of 120 seconds and below, the degree of mixing between the BGA SAC ball alloy and the Sn-Pb solder paste was less than 100 percent for packages with a ball pitch of 0.8mm or greater. Depending on package size, the peak reflow temperature was observed to have a significant impact on the solder joint microstructural homogeneity. The influence of reflow process parameters on solder joint reliability was clearly manifested in the Weibull plots. This paper provides a discussion of the impact of various profiles' characteristics on the extent of mixing between SAC and Sn-Pb solder alloys and the associated thermal cyclic fatigue performance.

Key words: Pb-free BGA, Sn-Pb, mixed solder alloy, backward process.

Introduction
The tin-lead (Sn-Pb) component availability issue has led many companies to consider using Pb-free Sn-Ag-Cu (SAC) BGA components in their Sn-Pb surface mount assembly processes. There has been considerable discussion around the long-term solder joint reliability of this so-called "mixed alloy" processing, which has not yet been characterized completely.

Several research papers [1-25] have demonstrated the significant impact that the presence of Pb can have on the reliability of Pb-free BGA solder joints assembled using Sn-Pb solder alloy. For example, addition of minute concentrations of Pb into a Pb-free SAC solder alloy has been reported [5] to appreciably reduce the fatigue life of the SAC-rich solder joint under thermo-mechanical fatigue tests. The work by Choi et al., 2001 [5] attributed the reduced fatigue resistance of the SAC solder joint to the formation of a low melting ternary alloy of 62.5wt.%Sn-1.35wt.%Ag-36.15wt.%Pb with a melting point of 178°C.

Hua et al., 2003 [6,7] reported that complete melting of the Sn-Ag-Cu (SAC) BGA solder ball followed by full mixing of the Pb-free SAC melt with the Sn-Pb solder paste melt is critical to board-level solder joint reliability. To ensure complete melting of the SAC solder ball would require the peak reflow temperature to be substantially increased beyond that of the eutectic Sn-Pb solder paste melting point. However, increasing the peak reflow temperature may be detrimental to low temperature rated components that are part of an assembly with the Sn-Ag-Cu BGA components.

In 2005, Snugovsky et al. reported [9, 10] that a complete mixing of SAC and Sn-Pb solder alloys may be achieved at a temperature lower than the liquidus temperature of Pb-free SAC solder balls. This temperature depends on solder ball alloy composition, SAC solder ball/Sn-Pb solder paste ratio, dwell time, and component size. Further, it was reported that the solder joint fatigue life was component dependent and, in the case of complete mixing of the solder alloys, it may be better, equal, or worse than the fatigue life of similar Sn-Pb assemblies. One year later (in 2006), McCormick et al.[11] reported building reliable solder joints of Pb-free SAC solder alloy mixed with Sn-Pb solder paste for some specific types of Pb-free BGAs packages. The assembly conditions in the work they conducted were equivalent to those of the typical Sn-Pb assembly process.

The work by Snugovsky et al., 2004 [12] on the evolution of the microstructure of mixed Sn-Pb/Pb-free SAC BGA solder joints reported the presence of the low melting Sn-Ag-Pb eutectic ternary alloy in the solder joints. This study reported that the presence of Ag_3Sn IMC particulates in the solder joint matrix correlated with enhanced solder joint reliability. Further, regarding the microstructure of mixed solder joint and its impact on solder joint strength, an earlier study done by Oliver et al., 2002 [13] attributed the reduction in fatigue resistance of the mixed alloy lead-free Sn-Ag-Cu in Sn-Pb solder joint to the Pb precipitates residing at the Sn grain boundaries. These precipitates were found to have contributed to early grain boundary fractures.

Based on the research cited above, it is clear that an understanding of the factors that affect solder joint reliability when a Pb-free SAC ball alloy is mixed with Sn-Pb solder paste is critical in determining a reflow process suitable for lead-free SAC BGAs built using Sn-Pb solder paste and process parameters. The investigation discussed in this paper, conducted under the auspices of the International Electronics Manufacturing Initiative (iNEMI) consortium, is an attempt to provide further understanding of the solder joint reliability for Pb-free BGAs assembled using Sn-Pb solder paste and within the low peak temperature limits required under the eutectic Sn-Pb solder paste specifications for package size up to $45mm^2$ at a pitch of 1.27mm.

Experimental Design

Based on the results from previously published studies [1-25], the iNEMI Board Assembly Technology Integration Group launched the "Pb-free BGAs in Sn-Pb Assemblies Project" in order to address some of the gaps identified when assembling SAC BGAs using Sn-Pb solder paste within the reflow conditions dictated by the Sn-Pb assembly process. This project investigated the impact of SAC BGA ball pitch and BGA package size, SAC ball volume, reflow process parameters and PCB surface finishes on the reliability of Pb-free BGA package solder joints built using Sn-Pb solder alloy with the typical eutectic Sn-Pb solder paste reflow conditions. Following are specifications for each of the factors selected to investigate the reliability of mixed alloy solder joints:

1) Package Size/Pitch: Package body size ranging from 8 to 45 mm^2 and the corresponding pitch size ranging from 0.5mm to 1.27 mm.
2) Solder Paste Volume: Standard stencil aperture opening design of 10% reduction and 1:1 (or 100%).
3) Peak Reflow temperature (PRT): A peak reflow temperature of 210°C and 215°C with Sn-Pb paste and 235°C for Pb-free solder paste (control sample).
4) Time above Liquidus (TAL): Time above liquidus of 60, 90 and 120 seconds.
5) Surface Finish: Surface finish of copper OSP and ENIG.

Using the factors listed above, a simple design of experiment was created as shown in Table 1. The matrix contains eight test cells defined by variations in assembly process flow, which were generated using five different processing conditions of TALs and peak temperatures (numbered 1 through 5 in Table 1).

Table 1: Assembly Test Matrix

Assembly Process Flow	Reflow Profile Number	BGA Ball Alloy	Solder Paste Alloy	Peak Temp. (°C)	Time Above Liquidus (sec)	Stencil Aperture Opening (%)
1 (Control)	1	Sn-Pb	Sn-Pb	210	60	90
2	1	Sn-Ag-Cu	Sn-Pb	210	60	90
3	2	Sn-Ag-Cu	Sn-Pb	210	90	90
4	3	Sn-Ag-Cu	Sn-Pb	210	120	90
5	1	Sn-Ag-Cu	Sn-Pb	210	60	100
6	2	Sn-Ag-Cu	Sn-Pb	210	90	100
7 (Control)	4	Sn-Ag-Cu	Sn-Ag-Cu	235	60	90
8	5	Sn-Ag-Cu	Sn-Pb	215	60	90

Experimental Materials

Four types of BGA packages were selected based on component body size, ball-to-ball pitch size, and ball diameter. The characteristics of the four packages are listed in Table 2.

Table 2: Component Characteristics

Component Designation	Package Body Size (mm^2)	Input/Output Pin Count	Ball Pitch (mm)	Ball Diameter (mm)
SBGA600	45 x 45	600	1.27	0.76
PBGA324	23 x 23	324	1.0	0.63
CABGA288	19 x 19	288	0.8	0.46
CTBGA132	8 X 8	132	0.5	0.3

BGA packages with both Pb-free and Sn-Pb ball alloys were used. The composition of the alloy used for the Pb-free BGA balls was Sn-4wt.%Ag-0.5wt.%Cu (labeled as SAC405) and that of the Sn-Pb BGA balls was the eutectic Sn-37wt.%Pb solder alloy. All packages had electrolytic nickel-gold as the base surface finish. Figure 1 shows photographs of the bottom side (ball up) of all the components used in this study.

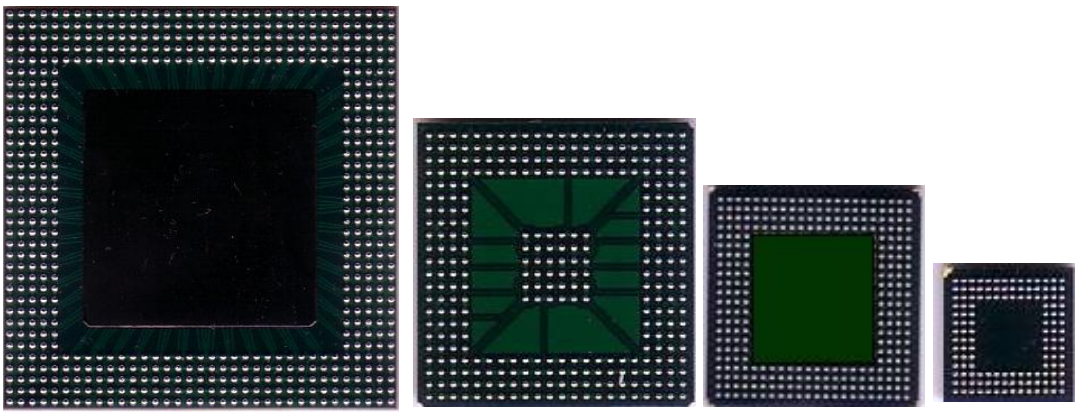

SBGA600 PBGA324 CABGA288 CTBGA132

Figure 1: Components, ball side up

The nominal dimensions of the test board used in this study are: 7″ x 4″ x 0.093″. The board contains 8 copper layers with 4 layers being ground, to assist with minimizing temperature gradient across the board during reflow. A laminate with a glass transition temperature (T_g) of 170°C and decomposition temperature (Td) of 340°C was chosen to ensure laminate robustness during processing and reliability testing.

A typical eutectic Sn-37wt.%Pb type-3 no-clean solder paste was used for the assembly. Similarly, a typical Sn-3.0wt.%Ag-0.5wt.%Cu type-3 no-clean solder paste was used for the Pb-free control assemblies.

Two stencils were used in this study. One stencil incorporated a standard 90% stencil aperture opening to the PCB pad size while the other had a 1:1 match to the PCB BGA test pads. All of the stencils had a thickness of 0.005″ and were laser cut and electropolished.

Assembly Procedure

A bare board was pre-drilled for thermocouple instrumentation. Two thermocouples per array package were used for profiling, placed along the diagonal line of the package PCB footprint. Once thermocouples were placed on the board, reflow profiles were created using a 10-zone convection reflow oven. A thermal gradient of 5°C or less was targeted across the board, with the largest package solder joint temperature being +0°C/-5°C of peak temperature. Figure 2 shows a reflow profile used for assembling the components with a target peak temperature of 210°C and a TAL of 60 seconds.

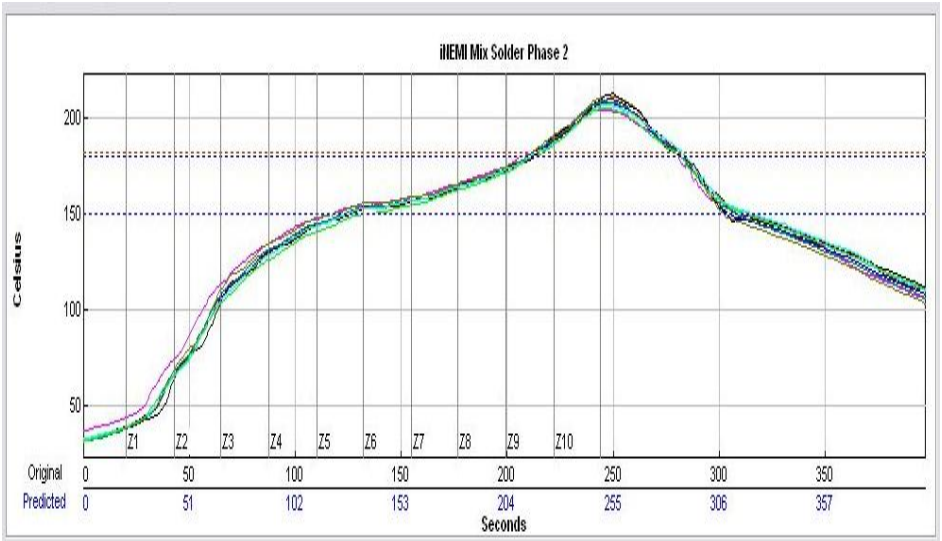

Figure 2: Representative reflow profile (PRT: 210°C; TAL: 60 seconds)

Standard solder paste print setup was used in this investigation. Several test prints were performed on sample boards to ensure proper paste release was achieved prior to any printing for the assembly build. Once the paste printing process was completed, reflow profiles were generated and first articles assembled for each "assembly flow process" test cell as given in Table 1. Remaining boards were assembled thereafter. A representative fully assembled test board is shown in Figure 3.

Figure 3: Representative assembled test board.

Accelerated Thermal Cycling (ATC) Testing Considerations

Assembled boards were tested using the IPC-9701A standard. The boards were subjected to a maximum of 3559 accelerated thermal cycles over the temperature range of -40°C to 125°C. The ramp rate was an average of 11°C per minute and the minimum solder joint dwell time was 10 minutes at the temperature extremes. The resistance changes were continuously monitored using a two-wire resistance monitoring system that recorded all resistance and temperature values at a scan interval of not more than 60 seconds. A failure was defined as five consecutive fails above 20% of the nominal resistance value. Table 4 presents the detailed test matrix including the number of assemblies tested. (Note that some test vehicles for vibration testing are included in Table 4, but only the thermal cycling data is discussed in this paper.)

Table 4: Assembly test matrix including the mechanical and accelerated thermal cycle test.

Assembly Process Flow	BGA Ball Alloy	Solder Paste Alloy	Peak Temp. (°C)	Time Above Liquidus (TAL) (seconds)	Stencil Aperture Opening	Number of Boards for Metallography Test (Vibration)		Number of Boards for ATC Testing (Range: 40°C to 125°C)	
						ENIG	OSP	ENIG	OSP
1(Control)	Sn-Pb	Sn-Pb	210	60	90	0	5	3	6
2	Sn-Ag-Cu	Sn-Pb	210	60	90	0	5	0	6
5	Sn-Ag-Cu	Sn-Pb	210	60	100	0	5	3	6
3	Sn-Ag-Cu	Sn-Pb	210	90	90	0	5	0	6
6	Sn-Ag-Cu	Sn-Pb	210	90	100	0	5	0	6
4	Sn-Ag-Cu	Sn-Pb	210	120	90	0	5	3	6
7(Control)	Sn-Ag-Cu	Sn-Ag-Cu	235	60	90	0	5	0	6
8	Sn-Ag-Cu	Sn-Pb	215	60	90	0	3	0	3
						0	38	9	45

ATC Reliability Results and Discussion

A summary of the thermal cycling results after the completion of 3559 testing cycles is shown in Table 5. At the conclusion of ATC testing, all of the smaller BGA components (CABGA288 and CTBGA132) had failed as indicated by the yellow highlighted boxes. The grey highlight in Table 5 shows that no CABGA288 and CTBGA132 packages were assembled under the assembly flow condition 8. The two green highlighted boxes show the number of SBGA600 packages assembled on OSP finished PCBs that failed. The green highlighted box under assembly process flow 1A shows that only 1 out of 18 SBGA600 packages with pure Sn-Pb solder joints failed while the green highlighted box under assembly process flow 7 shows that 4 out of 18 of the SBGA600 packages with pure SAC solder joints failed. The data in the clear/white highlighted boxes

represents packages that had not failed at the end of the ATC testing period. Interestingly, it is the largest packages, PBGA324 and SBGA600 with mixed solder alloy joints that displayed this characteristic. However, it is important to note also in Table 5 that under the assembly process flow 1B (packages assembled on ENIG finished PCBs), all the PBGA324 and SBGA600 packages failed. Another significant note from Table 5 is that 17 out of 18 PBGA324 packages built under the assembly flow 7 (pure SAC solder joints) failed.

Table 5: A summary of the accelerated thermal cycling test results showing the number of failed packages corresponding to package size, PCB surface finish and assembly process flow conditions (as given in column 1 of Table 4)

	Number of Failed Packages After 3559 ATC testing Cycles										
PCB Finish	OSP	ENIG	OSP	OSP	OSP	ENIG	OSP	ENIG	OSP	OSP	OSP
Assembly Process Flow	1A	1B	2	3	4A	4B	5A	5B	6	7	8
SBGA600	1/18	9/9	0/18	0/18	0/18	0/9	0/18	0/9	0/18	4/18	0/18
PBGA324	0/18	9/9	0/18	0/18	0/18	0/9	0/18	0/9	0/18	17/18	0/18
CABGA288	18/18	9/9	18/18	18/18	18/18	9/9	18/18	9/9	18/18	18/18	0
CTBGA132	18/18	9/9	18/18	18/18	18/18	9/9	18/18	9/9	9/9	18/18	0

Failure analysis of the SBGA600 package revealed solder joint cracks on both the PCB and the package interfaces that only extended about half-way through the solder joint interfaces. This failure mode is represented in the dye and pry mapping shown in Figure 4. Figure 5 shows an SEM image depicting the same failure mode. This failure mode could not be confirmed by electrical testing. Figures 4 and 5 represent the typical failures that were observed on the largest BGA packages.

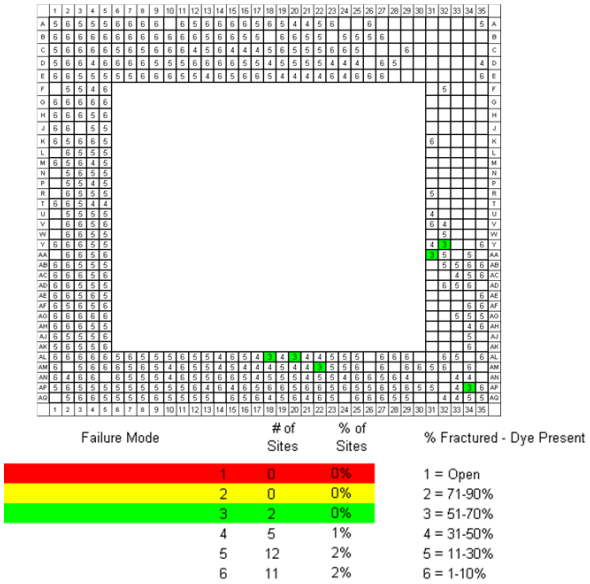

Figure 4: The Dye and Pry mapping for SBGA600 component showing the crack locations and percent fracture of the solder joints.

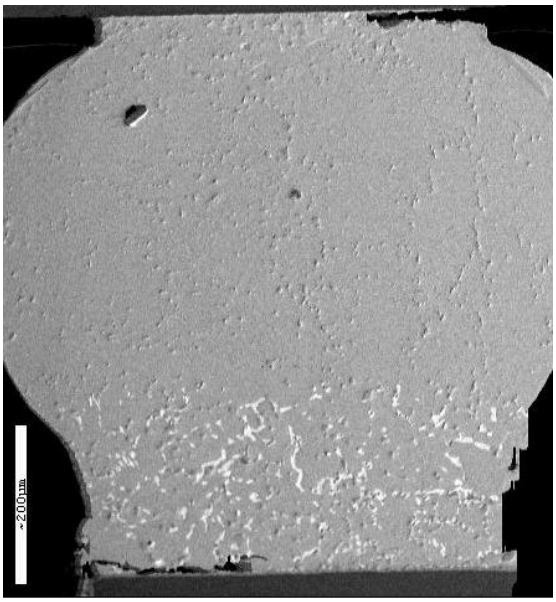

Figure 5: SEM image showing the typical solder joint fractures observed on the SBGA600package. These fractures could not be confirmed by electrical testing.

The failure data presented in Table 5 was further statistically analyzed using two-parameter Weibull models, but only the CTBGA132 and CABGA288 provided enough data for analysis. The next section discusses failure analysis data for these two packages.

Impact of Time above Liquidus Temperature (TAL)
A review of the solder joint reliability data for the CTBGA132 component assembled on an OSP-finished PCB using a peak temperature of 210^{o}C and a 90% stencil-to-pad opening for Sn-Pb paste deposition is discussed first.

In Figure 6, the impact of time above liquidus on solder joint reliability for the CTBGA132 package is shown. It was observed that increasing the TAL from 60 to 120 seconds correlated with improved solder joints reliability for this package. It was also noted that the 120 seconds TAL corresponded with the highest slope and the 60 seconds TAL corresponded with the smallest slope. From the results of the as-assembled solder joints reported elsewhere [23], all the TALs had shown complete or full mixing between Pb-free Sn-Ag-Cu and Sn-Pb solder alloys.

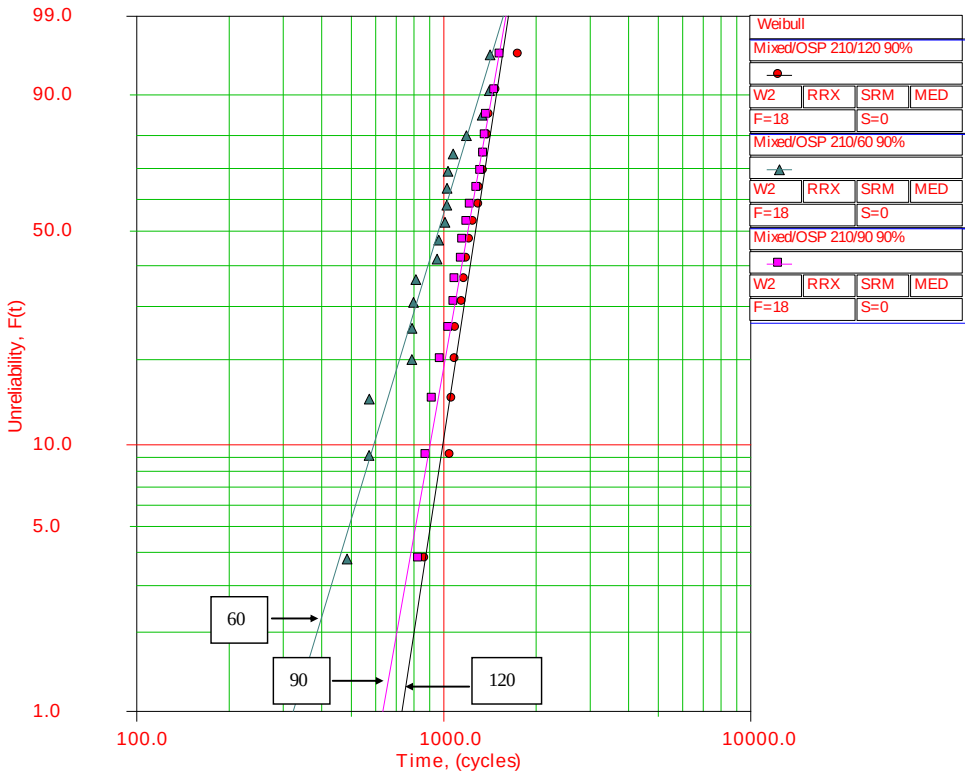

Figure 6: A Weibull plot showing the impact of the time above liquidus temperature on solder joint reliability for the CTBGA132 component.

Further, the CTBGA132 solder joint failure modes observed at the three different TALs were evaluated. In Figure 7, the failure mode observed for a package assembled using a 60-second TAL is shown. The failure was recorded only after 484 thermal cycles but the component was further cycled to 3010 cycles. Notable from Figure 7 is that 100% mixing between the Sn-Pb and the Sn-Ag-Cu solder alloys was obtained.

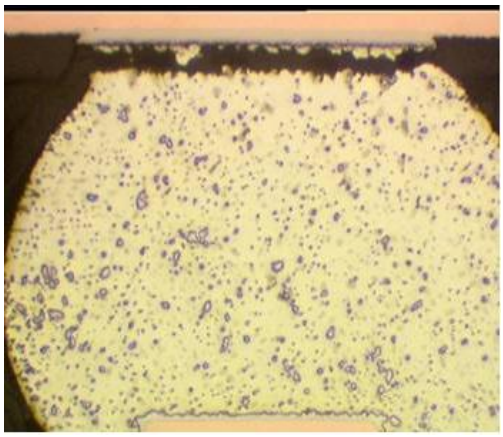

Figure 7: An optical image at 100x of a cross-section of CTBGA132 component solder joint that failed after 484 thermal cycles.

More detailed examination using scanning electron microscopy (SEM) of the solder joint microstructure revealed that mixing a SAC solder ball with Sn-Pb solder paste may not necessarily result in uniform microstructure. The component side microstructure often contains more Sn primary phase and less interdendritic Sn+Pb+Ag_3Sn+ eutectic as observed in Figure 8. This type of structure recystallizes more easily than those with the intermetallic particles at the grain boundaries and reduces reliability. The eutectic accumulation may occur at the board side causing an interfacial failure through the Pb-rich layer. This zonal microstructure formation is typical of an alloy with a wide pasty range solidifying in non-uniform heat dissipation

conditions. For SAC solder ball/Sn-Pb solder joints the minimum liquidus-solidus range is not narrower than 30°C [24, 25]. The freezing of mixed alloy begins with primary Sn dendrite formation. They preferably nucleate on the existing Sn crystals that may not completely dissolve in liquid solder or on Sn clusters that existed in liquid solder at the temperature very close to the solidus point. The solidification continues with the binary Sn-Pb and then ternary Sn+Ag_3Sn+Cu_6Sn_5 formation in interdendritic spaces toward the hottest part of the joint, which is more likely the board side.

Unfortunately, this level of microstructure examination was not applied to the as-assembled condition. After thermal cycling, it was difficult to separate microstructure evaluation during thermal cycling from the initial microstructure. Nevertheless, increasing the time above liqiudus allows for improved uniformity of liquid solder, dissolving the last portion of Sn phase, destroying some clusters and reducing temperature gradient across the solder joints.

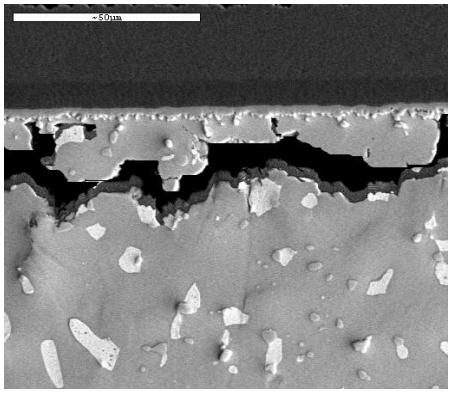

Figure 8: Cross-section SEM image of CTBGA132 component solder joint recorded to have failed after 981 thermal cycles.

The Weibull plots for CTBGA132 components are shown in Figure 9 and the results are summarized in the histogram in Figure 10. These figures present data comparing the solder joint reliability of the Sn-Pb/Sn-Ag-Cu mixed alloy solder joints to the "pure" Sn-Pb and Sn-Ag-Cu solder joints as a function of time above liquidus with a 90% stencil opening for paste release. The solder joint reliability of mixed SAC ball/Sn-Pb assembled at 120 seconds above liquidus temperature (TAL) outperforms the "pure" Sn-Pb joints and the reliability of mixed solder joints is as good as that of "pure" Sn-Ag-Cu Pb-free solder joints. From the foregoing results, it was observed that increased TAL during assembly of the CTBGA132 component correlated with improved solder joint reliability.

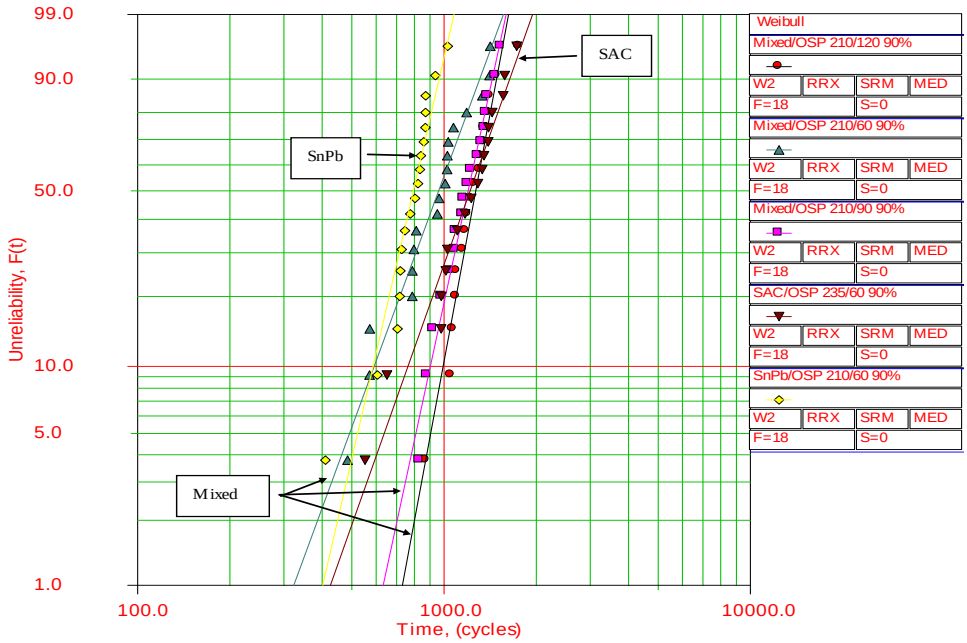

Figure 9: A Weibull plot showing the reliability of mixed alloy (Sn-Pb and Sn-Ag-Cu) solder joints, the "pure" Sn-Pb and "pure" Sn-Ag-Cu solder joints as a function of the time above liquidus for the CTBGA132 component.

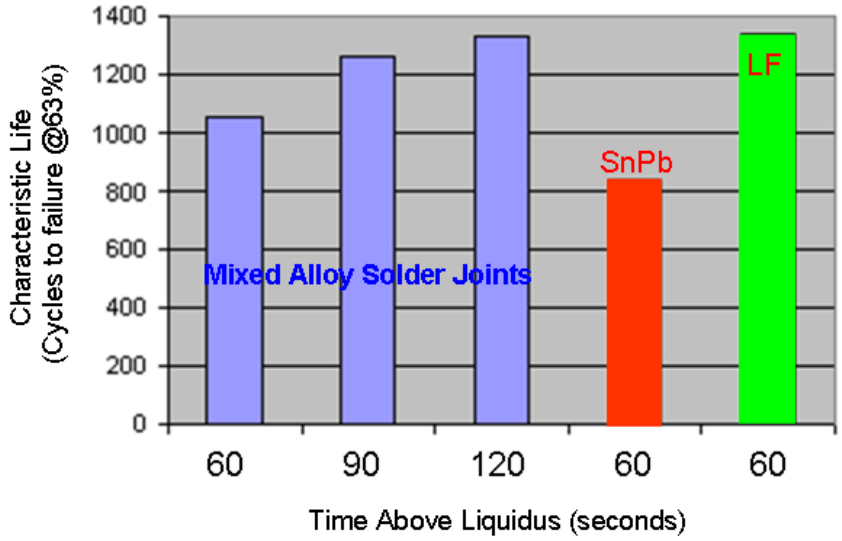

Figure 10: Impact of time above liquidus on the reliability of mixed solder joints for the CTBGA132 component. Increasing the TAL correspond to increased characteristic life.

An optical image of a cross-section of a Sn-Pb/Sn-Ag-Cu mixed alloy solder joint assembled with a TAL of 60 seconds, a peak temperature of 210°C and a 90% stencil opening is shown in Figure 11. The solder joint failed after 679 thermal cycles but were cut out from the test vehicle after 3010 thermal cycles. A typical failure mode was observed on the component/solder interface side along the microstructural coarsened band.

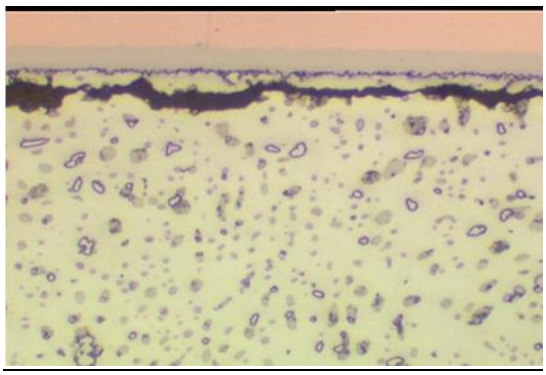

Figure 11: Failure mode observed for SAC/Sn-Pb mixed solder joint after 679 thermal cycles.

The impact of time above liquidus on the characteristic life for the CABGA288 component is illustrated in Figure 12. The data in this graph shows that increased TAL does not necessarily correspond to improved solder joint reliability.

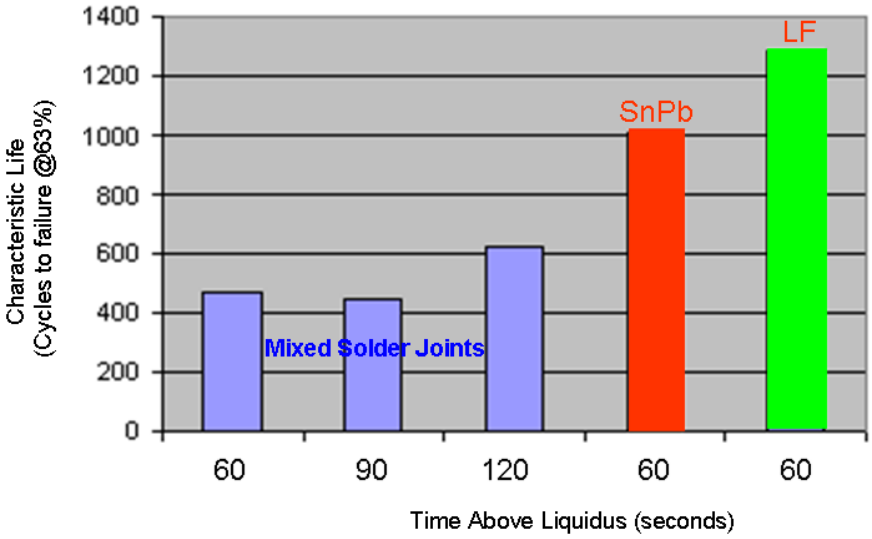

Figure 12: Impact of time above liquidus on the reliability of mixed solder joints for the CABGA288 component. Increasing the TAL does not improve solder joint reliability.

The trend of the data displayed in Figure 12 is thought to correlate to the extent of mixing observed between the Sn-Pb and the SAC solder alloys. In the case of the CABGA288 component, all of the TAL testing parameters used did not provide homogenized mixing between the alloys, a necessary condition for improved reliability.

Surface Finish Effect

Boards with OSP copper and ENIG were assembled and subjected to accelerated temperature cycling to understand the reliability of mixed solder when used on copper and nickel surfaces. Figure 13 compares the impact of surface finish (OSP and ENIG surface finishes on copper pads) on solder joint reliability for the CTBGA132 package with mixed alloy solder joints and pure Sn-Pb controls. Important to note is that, for this component, the extent of SAC and Sn-Pb solder alloys mixing under all assembly process flow conditions was observed to be 100%. With this scenario, it was found that solder joint reliability was better when soldered directly to copper than when using ENIG for the mixed solder assemblies. Similar findings were also observed on the control Sn-Pb assemblies.

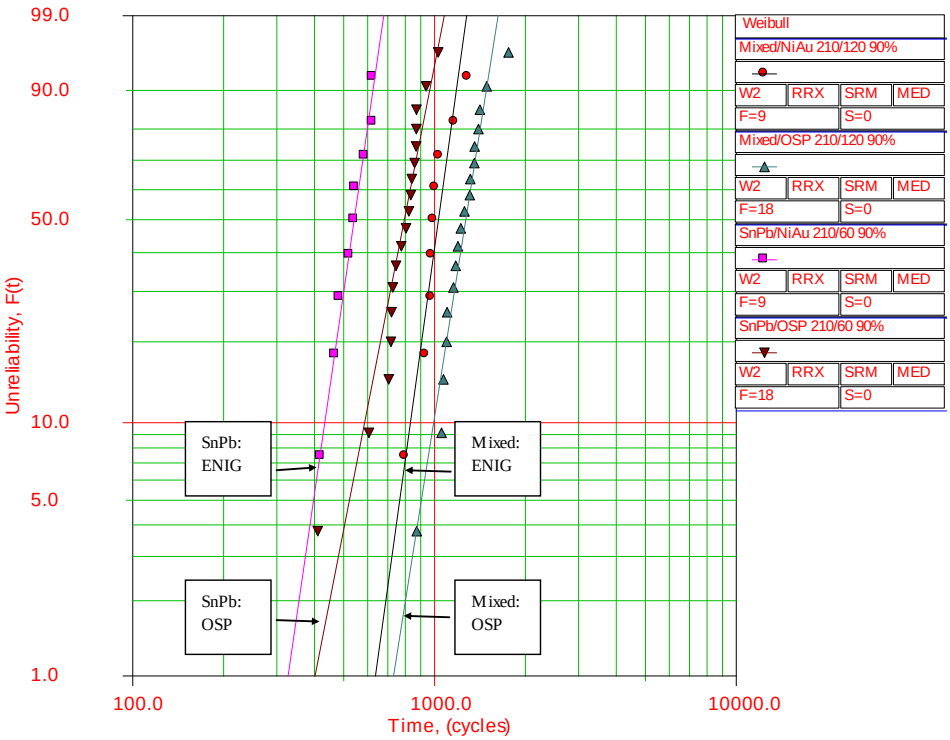

Figure 13: Weibull plot showing the impact of surface finish (OSP and ENIG surface finishes on copper pads) on solder joint reliability for the CTBGA132 package with mixed alloy solder joints and pure Sn-Pb controls.

In examining the CBGA288 package, the pure Sn-Pb had a similar trend to that observed for the CTBGA132, both for the OSP and ENIG finishes. However, under the mixed solder system when the extent of mixing is less that 100%, the ENIG surface finish has better performance than the OSP finished copper as depicted in the Figure 14.

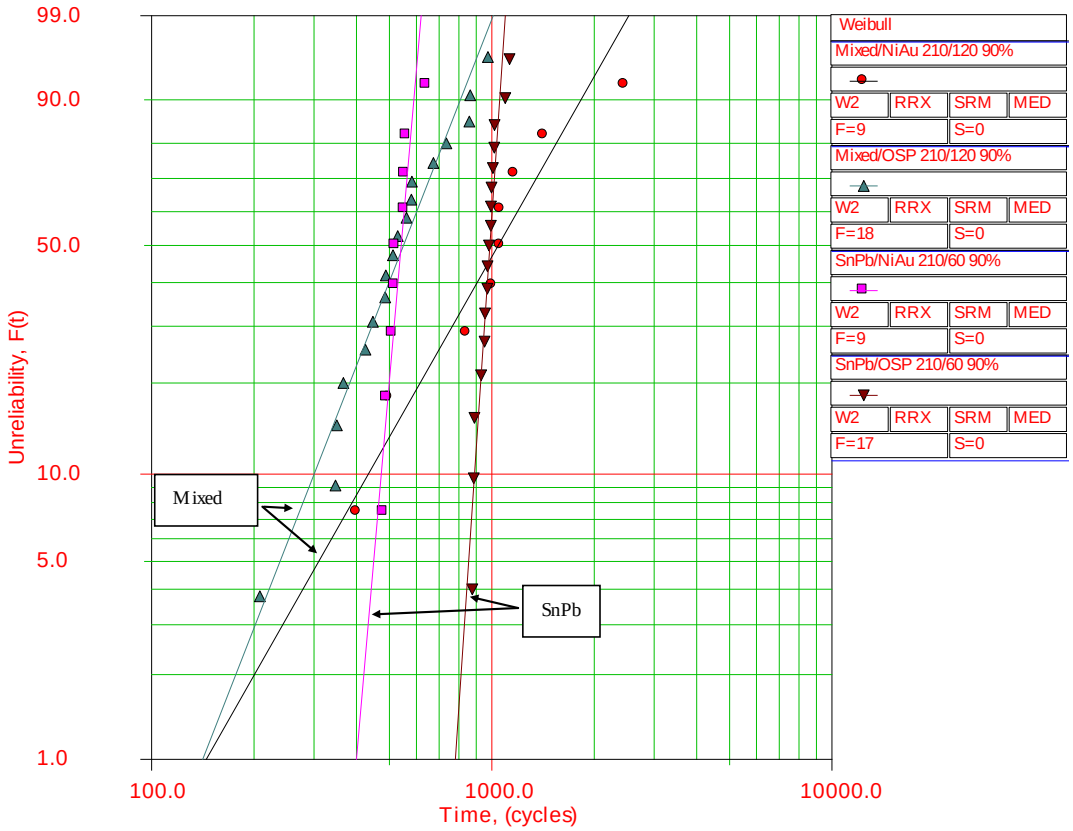

Figure 14: Weibull plot showing the impact of surface finish (OSP and ENIG surface finishes on copper pads) on solder joint reliability for the CABGA288 package with mixed alloy solder joints and pure Sn-Pb controls.

Failure analysis was performed for the mixed solder CTBGA132 attachment on copper OSP and ENIG surface finishes at 873 cycles and 980 cycles, respectively. For both finishes, the majority of the failures occurred within the bulk solder near the pad interface on the component side. The factures appeared to have been through the coarsened band indicating fatigue/creep failure. It was also noted that the mixed solder CTBGA132 with copper OSP surface finish had spalling intermetallics throughout the solder joint and a more homogenized solder structure.

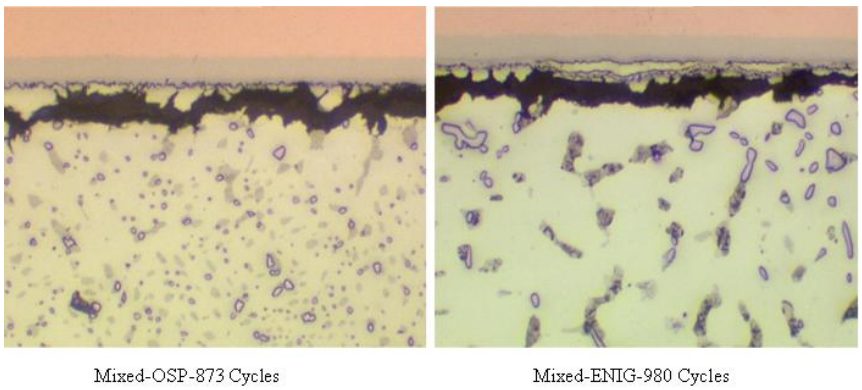

Figure 15: Photographs showing the failure modes observed on the mixed solder joints for the CTBGA132 package assembled on OSP and ENIG finished PCBs.

Peak Temperature

For the peak temperature comparison, only the PBGA324 and SBGA600 BGAs were assembled at two different peak temperatures to understand and compare the extent mixing of SAC and Sn-Pb solder alloys as well as reliability performance.

However, only minimal failures where observed for the PBGA324 and SBGA600 at the end of the 3559 ATC testing cycles. Due to the minimal failures observed, a comparison of peak temperature had not been performed at the time of writing this paper.

A Comparison of Mixed and Non-Mixed Solder Joints

When comparing mixed solder and pure Sn-Pb where solder paste volume is fixed, it was observed that having a higher level of mixing between the Pb-free solder ball and the Sn-Pb paste provided a higher solder joint reliability for the CTBGA132 and CBGA288 components.

In Figure 16, it is observed that for the CTBGA132 component, the mixed soldering conditions provided better reliability performance when compared to the pure Sn-Pb soldering conditions. The CTBGA132 in this test case had 100% mixed between the Pb-free solder ball and Sn-Pb paste. When examining the slope of the mixed solder at various times above liquidus, they appeared to be similar to the pure Pb-free system.

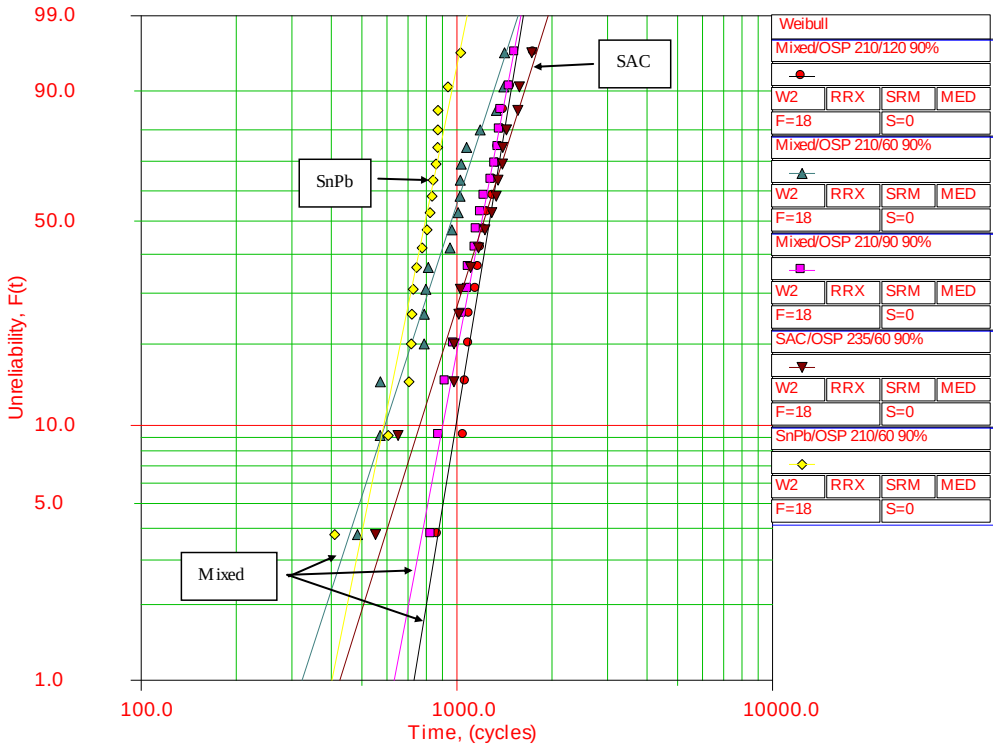

Figure 16: Weibull plot showing a comparison of the solder joint reliability between the mixed soldering conditions and the pure Sn-Pb and pure SAC soldering conditions on the CTBGA132 package.

When examining the reliability performance of the CBGA288 package, a similar trend to that observed in Figure 16 for the CTBGA132 package emerged. From Figure 17, it was found that the slope of the Weibull plots for the mixed solder testing conditions was similar to that of the pure Pb-free system. However, the reliability of the mixed solder joints was not as good as that of pure Sn-Pb or the pure Pb-free conditions. The extent of solder alloy mixing between the Pb-free and the Sn-Pb solder alloys was approximately 66%, 75% and 83% for 60, 90, and 120 seconds TAL respectively.

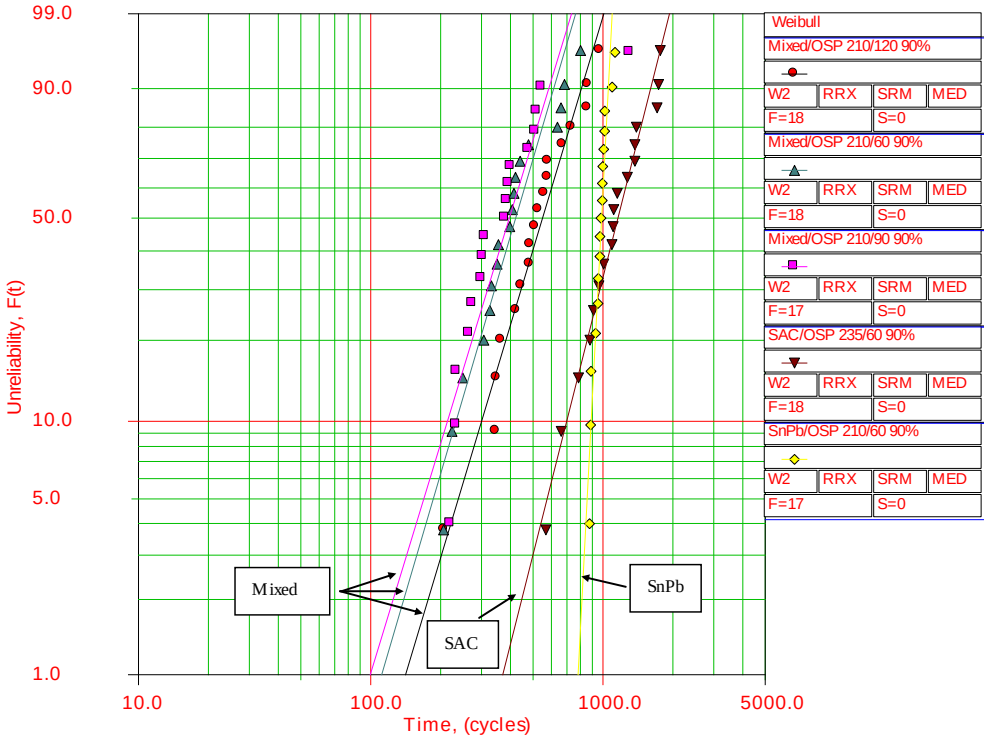

Figure 17: Weibull plot showing a comparison of the solder joint reliability between the mixed soldering conditions and the pure Sn-Pb and pure SAC soldering conditions on the CABGA288 package

Conclusions

At the time of publication of this paper, 3559 ATC test cycles were completed at a temperature range of -40°C to 125°C. The CTBGA132 (8mm and 0.5mm pitch) and the CABGA288 (19 mm and 0.8 mm pitch) packages showed a significant number of failures across all of the assembly test conditions, while no failures were recorded for the PBGA324 (23 mm and 1.0 mm pitch) and SBGA600 (45 mm and 1.27 mm pitch) packages for the mixed alloy assemblies. The following conclusions are drawn from this work:

- For the smallest, CTBGA132 package (8 mm and 0.5 mm pitch), all three TAL conditions had full solder alloys mixing. The solder joint reliability of the fully mixed test assemblies for all TALs (= 60, 90, and 120 seconds) exceeds that of Sn-Pb and is at least equal to that of pure SAC.
- For the larger, CABGA288 package (19 mm and 0.8 mm pitch), increasing the TAL does not provide complete solder alloy mixing. The solder joint reliability of all TALs tested (TAL = 60, 90, and 120 seconds) is less than that of both pure Sn-Pb and pure SAC. The longest TAL condition displayed a better solder joint reliability among the three TAL conditions.
- For the two largest packages, PBGA324 (23 mm and 1.0 mm pitch) and SBGA600 (45 mm and 1.27 mm pitch), despite lack of complete solder alloy mixing, the solder joint reliability was better than that of either “pure” Sn-Pb or “pure” SAC solder joints.
- In general, the OSP-copper had better performance than the ENIG surface finish. However, the failure locations were almost exclusively at the package side of the solder joint and within the bulk solder. At this time no microstructural correlation has been identified linking surface finish and improved or reduced reliability.
- Full Sn-Pb and SAC solder alloys mixing is not a sufficient condition to guarantee good reliability.
    - For small packages with low fatigue life requirements, full solder alloys mixing and homogeneous microstructure is required while for large packages with long fatigue/extended life requirement, full solder alloy mixing is not necessary for acceptable solder joint reliability.

Acknowledgements

The authors of this paper would like to thank the following project participants for their contribution to this work: Bill Barthel, Jasbir Bath, Russell Brush, Alex Chan, Indraneel Chatterji, Mike Davisson, Tim Dick, Dale Lee (for board design work), John Manock, Joe Menke, Dominic Peraro, Marianne Romansky, Brian Toleno, Aaron Unterborn, Jim Wilcox and Weidong Xie. Also, the authors acknowledge the support given by the process engineering team at Jabil who built the

assemblies as well as performed initial inspection of the assemblies. We would also like to thank the advanced technology team at Jabil who provided their expertise in initial failure analysis work. Finally, we would like to thank the management of the following companies for their support in providing the necessary wherewithal leading to the successful and timely completion of this work: Agilent Technologies, Alcatel-Lucent, Celestica Inc., Cisco Systems Inc., Henkel Technologies, IBM, Jabil, Plexus Corp., Sanmina-SCI Corporation and Solectron Corporation.

References

1). Hwang, J. S.; Environment-Friendly Electronics Lead-Free Technology, Electrochemical Publications, Great Britain, 2001.

2). Chung, C. K.; Aspandiar, R.; Leong, K. F.; Tay, C. S.; "The Interactions of Lead (Pb) in Lead-Free Solder (Sn/Ag/Cu) System"; Electronic Components and Technology Conference (ECTC), 2002.

3). Handwerker, C.; Bath, J., et al.; "NEMI Lead-Free Assembly Project: Comparison between PbSn and SnAgCu Reliability and Microstructures"; Proceedings of SMT International, 2003.

4) Rynemark, M.; Nylén, M.; Hutchinson, B.; "On the fatigue of solder subjected to isothermal cyclic shear"; Scripta Metallurgica et Materialia, Vol. 28, pp 349-353, 1993.

5) Choi, S.; Bieler, T. R.; Subramanian, K. N.; Lucas, J. P.; "Effects of Pb contamination on the eutectic Sn-Ag solder joint"; Soldering & Surface Mount Technology, 13/2, pp 26-29, 2001.

6). Zhu, Q.; Sheng, M.; Luo, L.; "The effect of Pb contamination on the microstructure and mechanical properties of SnAg/Cu and SnSb/ Cu solder joints in SMT"; Soldering & Surface Mount Technology, 12/3-2000, pp 19-23.

7). Hua, F.; Aspandiar, R.; Rothman, T.; Anderson, C.; Clemons, G.; Klier, M.; "Solder Joint Reliability of Sn-Ag-Cu BGA Components attached with Eutectic Pb-Sn Solder Paste;" Journal of Surface Mount Technology, Volume 16, Issue 1, pp 34-42, 2003.

8). Hua, F.; Aspandiar, R.; Anderson, C.; Clemons, G.; Chung, C-K.; Faizul, M.; "Solder Joint Reliability Assessment of Sn-Ag-Cu BGA Components Attached with Eutectic Pb-Sn Solder"; Proceedings of SMTA International Conference, Chicago, 2003.

9). Snugovsky, P.; Zbrzezny, A. R.; Kelly, M.; Romansky, M.; "Theory and Practice of Lead-Free BGA Assembly Using Sn-Pb Solder"; Journal of SMT, Vol. 6, Issue 1, 2005.

10). Snugovsky, P.; Zbrzezny, A. R.; Kelly, M.; Romansky, M.; "Theory and Practice of Lead-Free BGA Assembly Using Sn-Pb Solder"; CMAP International Conference on Lead-Free Soldering, Conference Proceedings, Toronto, May, 2005.

11). McCormick, H.; Snugovsky, P.; Bagheri, Z.; Bagheri, S.; Hamilton, C.; Riccitelli, G.; and Mohabir, R.; "Mixing metallurgy: Reliability of SAC Balled Area Array Packages Assembled Using SnPb Solder"; Pp 425-432, SMTAI, 2006.

12). Snugovsky, P.; Bagheri, Z.; Kelly, M.; "Solder Joint Formation with Sn-Ag-Cu and Sn-Pb Solder Balls and Pastes"; Proceedings of Electronic Component and Technology Conference, 2004.

13). Oliver, J., Rod, O., Nylén, M., Markou, C., "Fatigue Properties of Sn/3.5ag/0.7cu Solder Joints and Effects of Pb-Contamination"; Journal of SMT, Volume 15, Issue 4, 2002.

14). Kelly, M.; Snugovsky, P.; "Lead Free and Lead Bearing Solder Intermetallic Formation"; Proceeding of APEX Conference, 2003.

15). Zbrzezny, A.; Snugovsky, P.; Lindsay, T.; Lau, R.; "Reliability Investigation of Mixed BGA Assemblies"; IEEE Trans Elect Pkg Mfg, 29(3), pp 211-216, 2006.

16). Chatterji, I.; "Backward Compatibility, Are We Ready- A Case Study"; SMTA, Pp. 416-424, 2006.

17). Handwerker, C.; "Transitioning to Pb-free Assemblies, Circuits Assembly; March, 2005.

18). Abtew, M.; Kinyanjui, R.; Nuchsupap, N.; Chavasiri, T.; Yingyod, N.; Saetang, P.; Krapun, J.; and Jikratoke, K.,"Effect of Inert Atmosphere reflow and Solder Paste Volume on the Microstructure and Mechanical Strength of Mixed Sn-Ag-Cu and Sn-Pb Solder Joints"; SMTAI, 2006.

19). Hillman, D.; Wells, M.; Cho, K.; "The Impact of Reflowing a Pb-free Solder Alloy using a Tin/Lead Solder Alloy Reflow Profile on Solder joint Integrity"; CMAP International Conference on Lead-free Soldering, May 2005.

20). Nandagopal, B.; Chiang, D.; Teng, S.; Thune, P.; Anderson, L.; Jay, R.; and Bath, J.; "Study on Assembly, Rework Process, Microstructures and Mechanical Strength of Backward Compatible Assembly"; SMTA, pp 861-870, 2005.

21). McCormick, H.; Snugovsky, P., et al; "Pb-free Test Vehicle, Microstructure and ATC Behavior of SAC305 and SAC405 BGAs Assembled with SnPb Solder"; CMAP 2006.

22). Bath, J.; Sethuraman, S.; Zhou, X.; Willie, D.; Hyland, K.; Newman, K.; Hu, L.; Love, D.; Reynolds, H.; Kochi, K.; Chiang, D.; Chin, V.; Teng, S.; Ahmed, M.; Henshall, G.; Schroeder, V.; Nguyen, Q.; Maheswari, A.; Lee, M.; Clech, J. -P.; Cannis, J.; Lau, J.; Gibson, C.; "Reliability Evaluations of Lead-Free SnAgCu PBGA676 Components Using Tin-Lead and Lead-Free SnAgCu Solder Paste"; SMTA International, , pp 891-901, 2005.

23). Kinyanjui, R. and Chu, Q; "The Pb-Free Sn-Ag-Cu Ball Grid Array (BGA) Components in Sn-Pb Assembly Process; Process Characterization and Solder Joint Reliability", SMTA International Conference and Exhibition, Orlando, FL., October 9-11, 2007

24) Smith, B.; P. Snugovsky, M. Brizoux and A. Grivon, "Industrial Backward Solution for Lead Free Exempted AHP electronic Products, Part 2: Process Technology Fundamentals and Failure Analysis", APEX/IPC 2008 Conference.

25) Snugovsky, P; McCormick, H.; Bagheri, S.; Bagheri, Z.; Hamilton, C. and Romansky, M.; "Microstructure, Defects and Reliability of Mixed Pb-free/SnPb Assemblies", TMS 2008 Conference.